NUMERICAL STUDY OF PARTICLE, BUBBLE MOVEMENTS AND TUBE EROSION IN GAS FLUIDIZED BEDS

Alexandre M. S. Costa, amscosta@uem.br
Flávio C. Colman
Gabriel Lucas Foleiss
Julio C. D. Oliveira
Márcio Higa
Universidade Estadual de Maringá Av. Colombo 5790, bloco 104 , Maringá, PR, 87020-900

Abstract. *A numerical study based on a gas-solid eulerian-eulerian two fluid model has been conducted to predict bed fluid dynamics in face of immersed tubes. Our modeling is carried out using the open-source code MFIX. The two dimensional circular tubes' geometry is effected using stretched grids and using the cartesian cut-cell feature. The study is acquitted to investigate the geometric effect and main physical model parameters influence on the numerical results. The erosion model used is based on the monolayer energy dissipation model which assumes that the rate of available energy for erosion close to a surface is a constant fraction of the kinetic energy dissipation by the solids particles. In the geometric study, we focused on the variation of the ratio tube diameter to bed vertical wall spacing, tube location from the bottom of the bed, bounded and unbounded (periodic) walls. It was verified that the when the tubes are immersed in the bed, they acted as bubble splitters and deviators. It can be seen from results that the space between the immersed tubes and walls changes the dynamics of gas-solid flow above the obstacle. For the bounded bed, the bubble raising movement is concentrated in the center of the bed. For the unbounded domain, immersed tubes act like a perforated plate distributor for the bed dynamics above them. For the obstacle placed initially above the freeboard, greater contact time with large bubbles, that completely involves the tube was verified. For all cases, the immersed tubes affected the coalescence process initiated below of them. Different boundary conditions in the surface of the tubes were also investigated, specifically, slip and non-slip conditions for the gas and solid phases. The results predicted for the time-averaged rate for erosion was 60 % larger than for the non-slip condition. Following, the outcome of the two main parameters from the physical model was explored: solid stress models and drag relationship between the two phases. By his turn, solid stress models are used to predict the behavior of the solid phase in the kinetic and frictional regime. Ensuing, the following effects were investigated: transition from frictional to colisional regimes, constant solid phase viscosity in the kinetic regime, no solids viscosity in the frictional regime. The results for the time averaged rate for erosion predicted for different blending models of transition was the same. The maximum rate for erosion predicted using constant viscosity was half of variable viscosity model. For the lack of frictional viscosity, the maximum value of the rate for erosion was a fourth of the values predicted for the frictional viscosity usage. Except for the no frictional viscosity model, which predicted maximum values in the sides of the tubes, all the other models for solid stress predicted maximum value in the bottom side of the tube. Finally, for all the drag models investigated, the magnitude of the maximum values of the rate for erosion was the same, with the higher values occurring in the bottom side of the tube.*

Keywords*: fluidized bed, computational fluid dynamics, MFIX*

1. INTRODUCTION

Fluidized beds are widely used in combustion and chemical industries. The immersed tubes are usually used for enhancement of heat transfer or control of temperature in fluidized beds. By his turn, tubes subjected to the solid particle impact may suffer severe erosion wear. Many investigations have been devoted to erosion in tubes immersed in fluidized beds on the various influencing factors (cf. Lyczkowski and Bouillard, 2002). As pointed by Achim et al. (2002), the factors can be classified as particle characteristics, mechanical design and operating conditions.

Some previous experimental studies have focused on bubble and particle behaviors (Kobayashi et al., 2000, Ozawa et al., 2002), tube attrition, erosion or wastage (Bouillard and Lyczkowski, 1991; Lee and Wang, 1995; Fan et al., 1998; Wiman, 1994), heat transfer (Wong and Seville, 2006, Wiman and Almstedt, 1997) and gas flow regimes (Wang et. al, 2002).

Previous numerical studies were also performed using different CFD codes. Recently He et al. (2009, 2004), using the K-FIX code adapted to body fitted coordinates investigated the hydrodynamics of bubbling fluidized beds with one to four immersed tubes. The erosion rates predicted using the monolayer kinetic energy dissipation model were compared against the experimental values of Wiman (1994) for the two tube arrangement. The numerical values were three magnitudes lower than the experimental ones. Also employing a eulerian-eulerian model and the GEMINI numerical code, Gustavsson and Almstedt (2000, 1999) performed numerical computations and comparison against experimental results (Enwald et. al., 1999). As reported for those authors, fairly good qualitative agreement between the

experimental and numerical erosion results were obtained, and the contributions to the erosion from the different fluid dynamics phenomena near the tube were identified.

In the present study, we revisit the phenomena of the imersed tube in a gas fluidized bed with a single imersed tube employing the eulerian-eulerian two fluid model and the MFIX code. The purpose of the numerical simulations are to compare and explore some effects not previously investigated in the above mentioned references.

2. TWO FLUID AND EROSION MODELS

The mathematical model is based on the assumption that the phases can be mathematically described as interpenetrating continua; the point variables are averaged over a region that is large compared with the particle spacing but much smaller than the flow domain (see Anderson, 1967). A short summary of the equations solved by the numerical code in this study are presented next. Refer to Benyahia et al. (2006) and Syamlal et al. (1993) for more detailment.

The continuity equations for the fluid and solid phase are given by :

$$\frac{\partial}{\partial t}\left(\varepsilon_f \rho_f\right) + \nabla\bullet\left(\varepsilon_f \rho_f \vec{v}_f\right) = 0 \tag{1}$$

$$\frac{\partial}{\partial t}\left(\varepsilon_s \rho_s\right) + \nabla\bullet\left(\varepsilon_s \rho_s \vec{v}_s\right) = 0 \tag{2}$$

In the previous equations ε_f, ε_s, ρ_f, ρ_s, $\vec{v}_f$ and $\vec{v}_s$ are the volumetric fraction, density and velocity field for the fluid and solids phases..

The momentum equations for the fluid and solid phases are given by:

$$\frac{\partial}{\partial t}\left(\varepsilon_f \rho_f \vec{v}_f\right) + \nabla\bullet\left(\varepsilon_f \rho_f \vec{v}_f \vec{v}_f\right) = \nabla\bullet\bar{\bar{S}}_f + \varepsilon_f \rho_f \vec{g} - \vec{I}_{fs} \tag{3}$$

$$\frac{\partial}{\partial t}\left(\varepsilon_s \rho_s \vec{v}_s\right) + \nabla\bullet\left(\varepsilon_s \rho_s \vec{v}_s \vec{v}_s\right) = \nabla\bullet\bar{\bar{S}}_s + \varepsilon_s \rho_s \vec{g} + \vec{I}_{fs} \tag{4}$$

$\bar{\bar{S}}_f$ $\bar{\bar{S}}_s$ are the stress tensors for the fluid and solid phase. It is assumed newtonian behavior for the fluid and solid phases, i.e.,

$$\bar{\bar{S}} = \left(-P + \lambda\ \nabla\bullet\vec{v}\right)\bar{\bar{I}} + 2\mu\ S_{ij} \equiv -p\ \bar{\bar{I}} + \bar{\bar{\tau}} \qquad S_{ij} = \frac{1}{2}\left[\nabla\vec{v} + \left(\nabla\vec{v}\right)^T\right] - \frac{1}{3}\nabla\bullet\vec{v} \tag{5}$$

In the above equation *P, λ, μ* are the pressure, bulk and dynamic viscosity, respectively.

In addition, the solid phase behavior is divided between a plastic regime (also named as slow shearing frictional regime) and a viscous regime (also named as rapidly shearing regime). The constitutive relations for the plastic regime are related to the soil mechanics theory. Here they are representated as :

$$p_s^p = f_1\left(\varepsilon^*, \varepsilon_f\right) \qquad \mu_s^p = f_2\left(\varepsilon^*, \varepsilon_f, \phi\right) \tag{6}$$

In the above equation ε^* is the packed bed void fraction and ϕ is the angle of internal friction.

A detailing of functions f_1 to f_9 can be obtained in Benyahia (2008).

On the other hand, the viscous regime behavior for the solid phase is ruled by two gas kinetic theory related parameters (e, Θ).

$$p_s^v = f_3\left(\varepsilon_s, \rho_s, d_p, \Theta, e\right) \qquad \mu_s^v = f_4\left(\varepsilon_s, \rho_s, d_p, \Theta^{1/2}, e\right) \tag{7}$$

The solid stress model outlined by Eqs. (6) and (7) will be quoted here as the standard model. Additionally, a general formulation for the solids phase stress tensor that admits a transition between the two regimes is given by :

$$\bar{\bar{S}}_s = \begin{cases} \phi\left(\varepsilon_f\right)\bar{\bar{S}}_s^v + \left[1-\phi\left(\varepsilon_f\right)\right]\bar{\bar{S}}_s^p & \text{if } \varepsilon_f < \varepsilon^* + \delta \\ \bar{\bar{S}}_s^v & \text{if } \varepsilon_f \geq \varepsilon^* + \delta \end{cases} \tag{8}$$

According to Pannala et al.(2009), two diferent formulations for the weighting parameter "ϕ" can be employed :

$$\phi(\varepsilon)=\frac{1}{1+\upsilon^{\frac{\varepsilon-\varepsilon^*}{2\delta\varepsilon^*}}} \qquad \phi(\varepsilon)=\frac{\mathrm{Tanh}\left(\frac{\pi\left(\varepsilon-\varepsilon^*\right)}{\delta\varepsilon^*}\right)+1}{2} \tag{9}$$

In the above equation the void fraction range δ and the shape factor υ are smaller values less than unity. It must be emphasized that when δ goes to zero and ϕ equals to unity, the "switch" model as proposed by Syamlal et al. (1993) based on the Schaeffer (1987) can be recovered.

On the other hand, the Srivastava and Sundaresan (2003), also called "Princeton model", can be placed on the basis of Eq. (9)

Also in equations (4) and (5) $\vec{I}_{fs}$ is the momentum interaction term between the solid and fluid phases, given by

$$\vec{I}_{fs}=-\varepsilon_s\nabla P_f-\beta\left(\vec{v}_s-\vec{v}_f\right) \tag{10}$$

There is a number of correlations for the drag coefficient β (Eqs. 11 to 16). The first of the correlations for the drag coefficient is based on Wen and Yu (1966) work. The Gidaspow drag coefficient is a combination between the Wen Yu correlation and the correlation from Ergun (1952). The Gidaspow blended drag correlation allows controlling the transition from the Wen and Yu, and Ergun based correlations. In this correlation the χ blending function was originally proposed by Lathowers and Bellan (2000) and the value of parameter C controls the degree of transition. From Eq. (14), the correlation proposed by Syamlal and O'Brien (1993) carries the advantage of adjustable parameters C_1 and d_1 for different minimum fluidization conditions. The correlations given in Eq. (15) and Eq. (16) are based on Lattice-Boltzmann simulations. For detailments of these last drag correlations refer to the works by Benyahia et al. (2006) and Wang et al. (2010).

$$\beta_{\text{Wen-Yu}}=\frac{3}{4}C_D\frac{\rho_f\varepsilon_f\varepsilon_s\left|\vec{v}_f-\vec{v}_s\right|}{d_p}\varepsilon_f^{-2.65} \qquad C_D=\begin{cases}\dfrac{24}{\mathrm{Re}}\left(1+0.15\,\mathrm{Re}^{0.687}\right) & \mathrm{Re}<1000\\ 0.44 & \mathrm{Re}\geq 1000\end{cases} \qquad \mathrm{Re}=\frac{\rho_f\varepsilon_f\left|\vec{v}_f-\vec{v}_s\right|d_p}{\mu_f} \tag{11}$$

$$\beta_{\text{Gidaspow}}=\begin{cases}\beta_{\text{Wen-Yu}} & \varepsilon_f>0.8\\ \beta_{\text{Ergun}}=\dfrac{150\,\varepsilon_s\left(1-\varepsilon_s\right)\mu_f}{\varepsilon_f d_p^2}+\dfrac{1.75\,\rho_f\varepsilon_s\left|\vec{v}_f-\vec{v}_s\right|}{d_p} & \varepsilon_f\leq 0.8\end{cases} \tag{12}$$

$$\beta_{\text{Gidaspow-blended}}=\chi\,\beta_{\text{Wen-Yu}}+\left(1-\chi\right)\beta_{\text{Ergun}} \qquad \chi=\frac{\tan^{-1}\left(C\,\left(\varepsilon_f-0.8\right)\right)}{\pi}+0.5 \tag{13}$$

$$\beta_{\text{Syamlal-OBrien}}=\frac{3}{4}\frac{\rho_f\varepsilon_f\varepsilon_s}{V_r^2 d_p}\left(0.63+4.8\sqrt{\frac{V_r}{\mathrm{Re}}}\right)^2\left|\vec{v}_f-\vec{v}_s\right|$$

$$V_r=0.5A-0.03\,\mathrm{Re}+0.5\times\sqrt{\left(0.06\,\mathrm{Re}\right)^2+0.12\,\mathrm{Re}\,\left(2B-A\right)+A^2} \tag{14}$$

$$A=\varepsilon_f^{4.14} \qquad B=\begin{cases}C_1\varepsilon_f^{1.28} & \varepsilon_f\leq 0.85\\ \varepsilon_f^{d_1} & \varepsilon_f>0.85\end{cases}$$

$$\beta_{\text{Hill-Koch-Ladd}}=18\mu_f\left(1-\varepsilon_s\right)^2\varepsilon_s\frac{F}{d_p^2} \qquad F=f_9\left(F_0,F_1,F_2,F_3\right) \tag{15}$$

$$\beta_{\text{Beestra}}=180\frac{\mu_f\varepsilon_s^2}{d_p^2}+18\frac{\mu_f\varepsilon_f^3\varepsilon_s\left(1+1.5\sqrt{\varepsilon_s}\right)}{d_p^2}+0.31\frac{\mu_f\varepsilon_s\,\mathrm{Re}}{\varepsilon_f d_p^2}\frac{\left[\varepsilon_f^{-1}+3\varepsilon_f\varepsilon_s+8.4\,\mathrm{Re}^{-0.343}\right]}{\left[1+10^{3\varepsilon_s}\,\mathrm{Re}^{-0.5-2\varepsilon_s}\right.} \tag{16}$$

For closing the model, a transport equation for the granular energy Θ provides a way of determine the pressure and viscosity for the solid phase during the viscous regime. Equation (5) is a transport equation for the granular energy Θ. Its

solution provides a way of determine the pressure and viscosity for the solid phase during the viscous regime. The terms κ_s γ and ϕ_{gs} are the granular energy conductivity, dissipation and exchange, respectively.

$$\frac{3}{2}\left[\frac{\partial}{\partial t}\varepsilon_s\rho_s\Theta + \nabla\bullet\rho_s\vec{v}_s\Theta\right] = \bar{\bar{S}}_s : \nabla\vec{v}_s - \nabla\bullet\left(\kappa_s\nabla\Theta\right) - \gamma + \phi_{gs} \tag{17}$$

$$\kappa_s = f_5\left(\varepsilon_s, \rho_s, d_p, \Theta^{1/2}, e, \beta\right) \qquad \gamma = f_6\left(\varepsilon_s, \rho_s, d_p, \Theta^{3/2}, e\right) \qquad \phi_{gs} = f_7\left(\varepsilon_s, \rho_s, d_p, \Theta, \left|\vec{v}_f - \vec{v}_s\right|, \beta\right) \tag{18}$$

In the algebraic approach, instead solving the full equation (6) , the granular energy is obtained by equating the first term on the right hand side with the dissipation term.

The model where Eqs. (5) to (8) and (17) are solved is the kinetic theory model, termed here as KTGF. Conversely, in the constant solids viscosity model (CVM) the solids pressure is defined as in Eq. (6) and the solids viscosity in either plastic and viscous regimes is set constant.

For erosion calculations in this work we use the monolayer energy dissipation model (Lyczkowski and Bouillard, 2002). In that model the kinetic energy dissipation rate for the solids phase in the vicinity of stationary immersed surfaces is related to erosion rate in m/s by multiplication with an appropriate constant. This constant is function of surface hardness, elasticity of collision and diameter of particles hitting the surface. The kinetic energy dissipation rate Φ_s in W/m^3 for the solids phase is given by :

$$\Phi_s = \left[\varepsilon_s \bar{\bar{\tau}}_s : \nabla\vec{v}_s + \beta\frac{\vec{v}_s^{\,2}}{2}\right] \tag{19}$$

4. NUMERICAL METHOD

MFIX (Multiphase Flow with Interphase eXchanges) is an open source CFD code developed at the National Energy Technology Laboratory (NETL) for describing the hydrodynamics, heat transfer and chemical reactions in fluid-solids systems. It has been used for describing bubbling and circulating fluidized beds, spouted beds and gasifiers. MFIX calculations give transient data on the three-dimensional distribution of pressure, velocity, temperature, and species mass fractions.

The hydrodynamic model is solved using the finite volume approach with discretization on a staggered grid. A second order accurate discretization scheme was used and superbee scheme was adopted for discretization of the convective fluxes at cell faces for all equations in this work. With the governing equations discretized, a sequential iterative solver is used to calculate the field variables at each time step. The main numerical algorithm is an extension of SIMPLE. Modifications to this algorithm in MFIX include a partial elimination algorithm to reduce the strong coupling between the two phases due to the interphase transfer terms. Also, MFIX makes use of a solids volume fraction correction step instead of a solids pressure correction step which is thought to assist convergence in loosely packed regions. Finally, an adaptive time step is used to minimize computation time. See Syamlal (1998) for more details.

Figure 1 portrays the domain for the numerical simulations and four circumferential angles. The numerical runs were based on a cartesian two-dimensional coordinate system. The grid employed after mesh refinement is depicted in Figure 2. Following Cebeci et al.(2005), a non-uniform stretched grid, which has fine spacing close to the surface and coarse spacing away from the surface, was employed. The computer used in the numerical simulations was a PC with OpenSuse linux and Intel Quad Core processor.

In this work, the parameters for controlling the numerical solution (e.g., under-relaxation, sweep direction, linear equation solvers, number of iterations, residual tolerances) were kept as their default values. Also, for setting up the mathematical model, when not otherwise specified the code default values were used.

For generating the numerical results and comparison with experimental results, we employed the parameters given in Table 1, referred here as baseline simulation. Moreover, for the baseline simulation we employed the Syamlal-O´Brien drag model, the standard solid stress model, and slip and non-slip condition for solid and gas phase, correspondingly. The previous set of models will be referred in the results section as baseline simulation models.

Table 1. Baseline input parameters for CFD

H = 1 m	D = 0.1 m
h = 0.5 m	ε_{mf} = 0.42
V_0 = 0.4 m/s	μ_f = 2.0 10^{-5} kg/m s
d = 0.02 m	ρ_f = 1.2 kg/m^3
s = 0.3 m	d_p = 400 μm

20 × 200	ρ_s =2000 kg/m^3
Simulation time : 20 s	

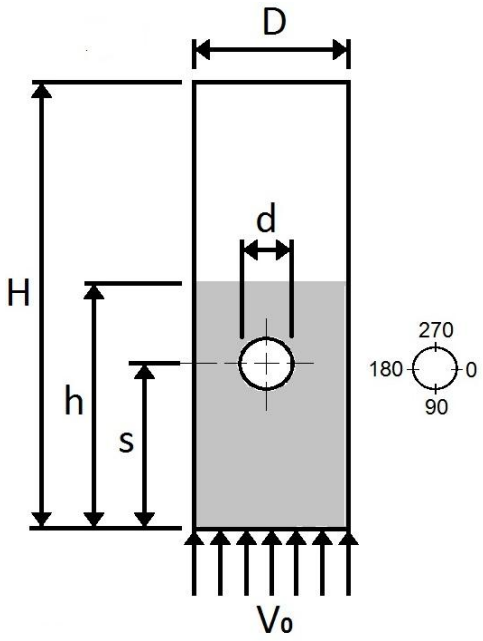

Figure 1. Bed scheme for numerical simulation and circumferential position angles

5. RESULTS AND DISCUSSION

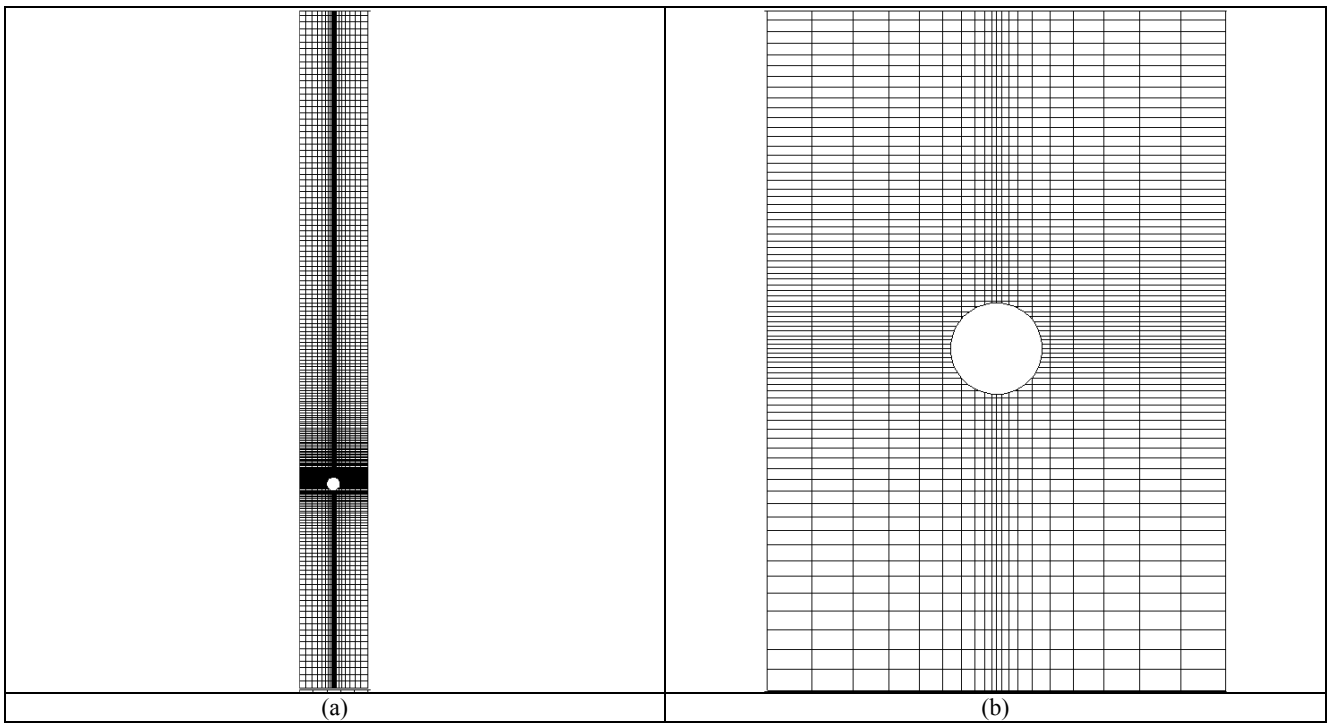

Figure 2. Stretched mesh and detailment around an obstacle

Figure 3 is a sampling plot showing the instantaneous solids velocities and gas volumetric fraction fields following a bubble passage around the obstacle. Analysis of Fig. (3) shows the bubble splitting mechanism taking place and the characteristic time scale for the bubble passage. After the bubble passage, the solid wake has higher solid velocity magnitude around the obstacle. From the simulated results, the highest values of kinetic energy dissipation rate occur

when the particle fraction suddenly changes from a low to a high value, which corresponds to the tube being hit by the wake of a bubble.

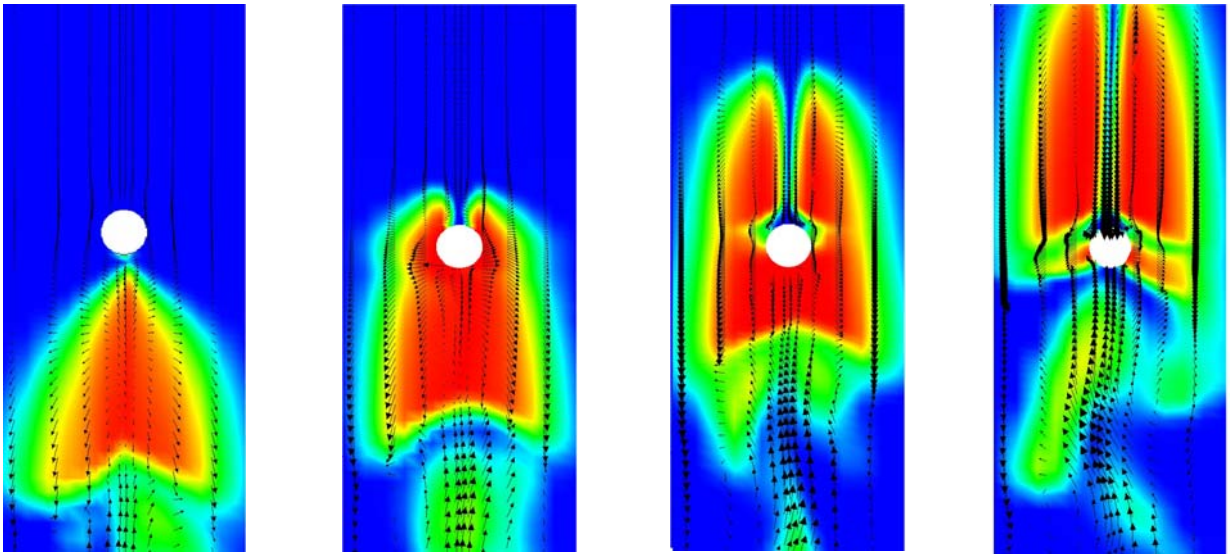

(a) 5.1 s (b) 5.2 s (c) 5.3 s (d) 5.4 s

Figure 3. Instantaneous voidage and solids velocity vector field

Figure 4 presents the time averaged kinetic energy dissipation as a function of circumferential position θ on the tube surface. As it would be seen from the majority of results the most severe dissipation occurs on the lower parts of the tube for an angle corresponding to 90 degrees. This fact is in agreement with experimental measured values of erosion from Wiman (1994). Analysis of results shows that, except for the BVK drag model, all the drag models predict the highest dissipation rate occurring at 90 degrees. The value predicted using the Syamlal-O'Brien drag model is the highest. There is a noticeable difference in the value of dissipation value between the Gidaspow and Gidaspow blend drag models, whereas the results by the Wen-Yu drag locate in the intermediate range. By his turn, the results by HYS and Koch-Hill models locates near the Wen-Yu values.

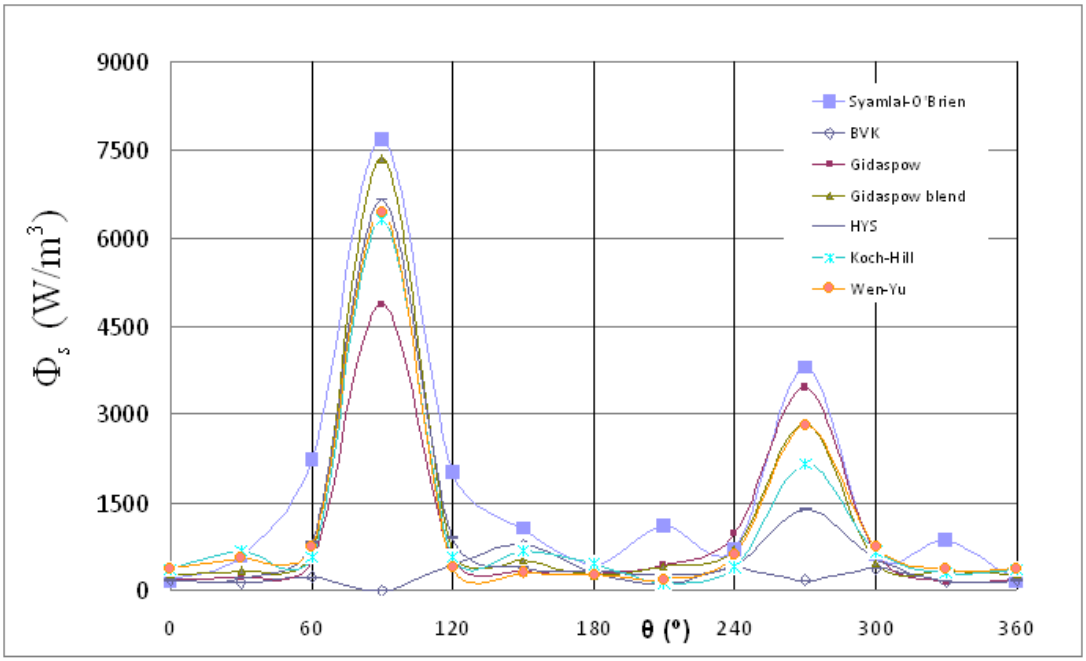

Figure 4. Time averaged kinetic energy dissipation predicted for different gas-solid drag models

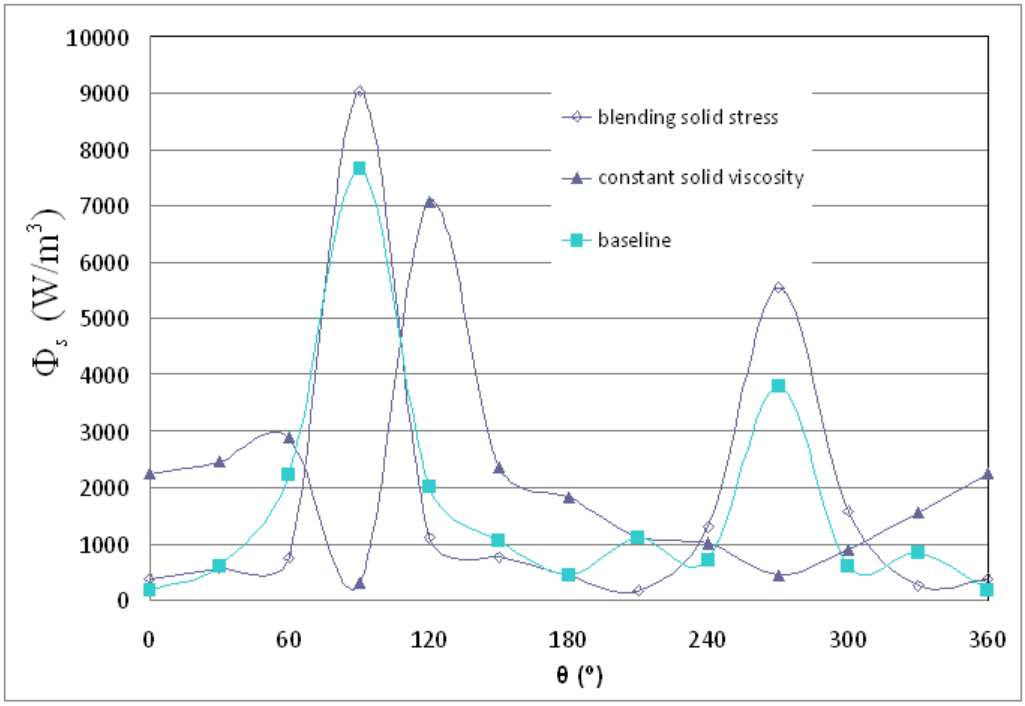

Figure 5. Time averaged kinetic energy dissipation predicted for different solid stress models

Figure 5 presents the result of kinetic energy dissipation for different solid stress models. As shown the peak values of the dissipation rate are close to 90 degrees for the model with (baseline) and without the blending function discussed in section 2. On the other hand, the value predicted by the constant solids viscosity model locates around 120 degrees, and it is inferior to the predicted by the solids kinetic energy theory.

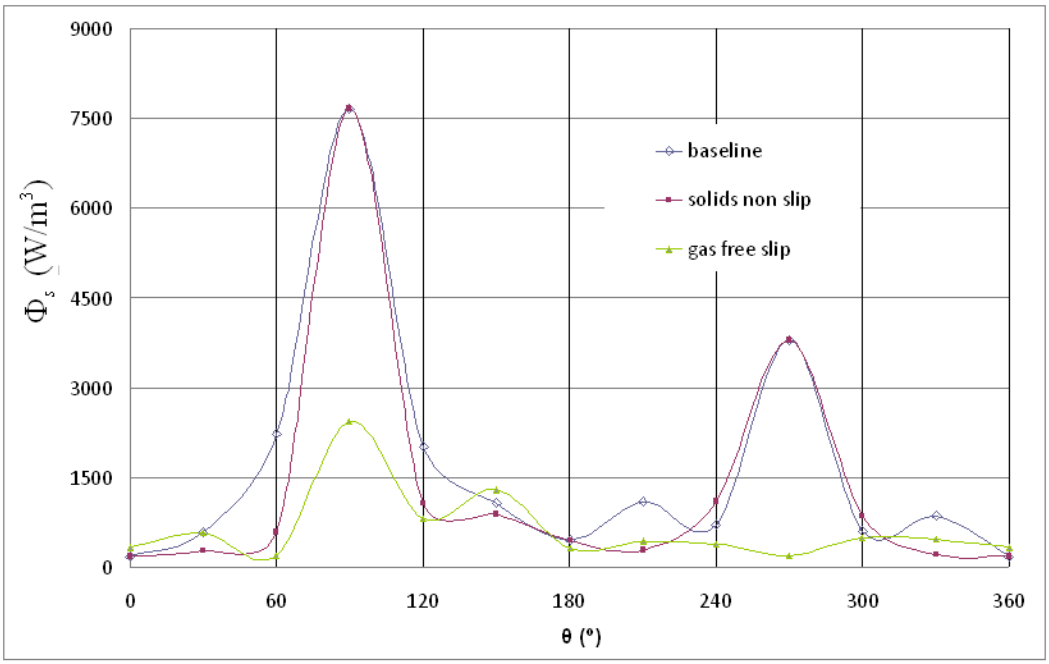

Figure 6. Time averaged kinetic energy dissipation predicted for different tube surface slip conditions

Figure 6 presents the result of kinetic energy dissipation for different tube surface slip conditions. The baseline case considers the free slip condition for the solids and non-slip condition for the gas. The peak values do not change when considering the solids with the non-slip condition. On the other hand, when considering slip conditions for both phases the value decreased. The above results, suggests the free slip condition for the gas phase on the surface of the tube plays an important role on the value of the kinetic energy dissipation.

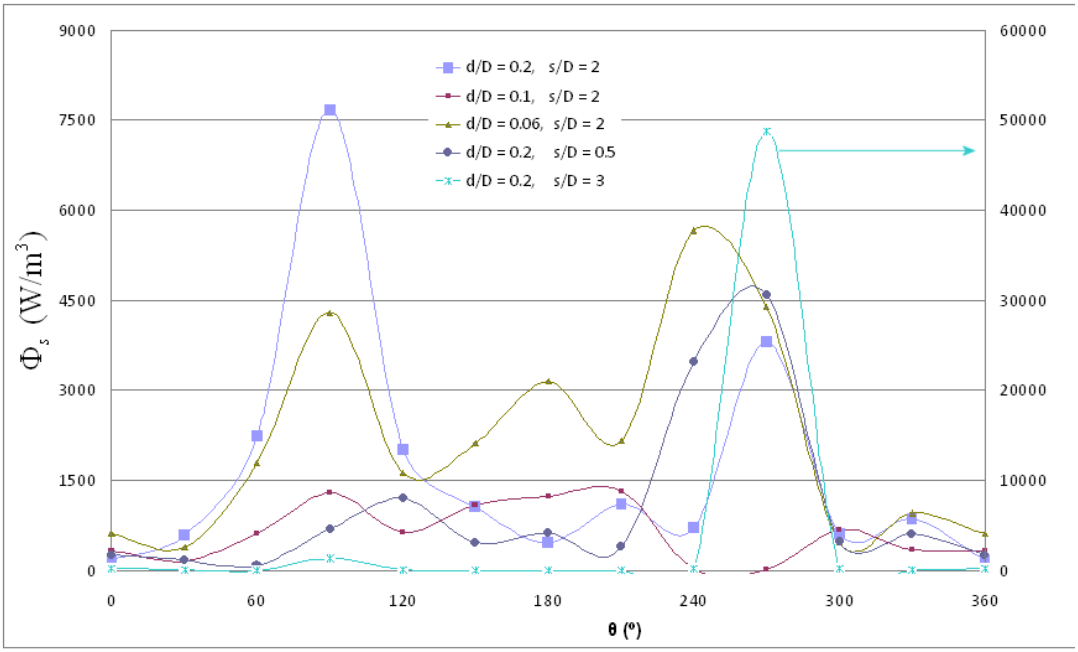

Figure 7. Time averaged kinetic energy dissipation predicted for different d/D ratios and s values

Figure 7 shows a comparison between the predicted values of energy dissipation for three different values of tube to bed width ratio d/D (0.2, 0.1 e 0.06) and different values of tube height s/D (3, 2 e 0.5). Analysis of Fig. 7 shows a decrease in the peak values for 90 degrees as the bed becomes larger (increasing d/D). The occurrence of the greatest peak values for an intermediate height s/D = 2 suggest the bubble size influences the dissipation. As verified by the simulation results bubbles grow with increasing height, this justifies the higher values for s/D = 2 (higher height) in comparison with s/D = 0.5 (smaller height). By his turn, the greater value for the highest tube height (s/D = 3) can be justified as the tube is located close to the freeboard, where there is intense solids moviment due to bubble erupts. This phenomena verified during the simulations also justifies the greater value occurrence in the top of the tube.

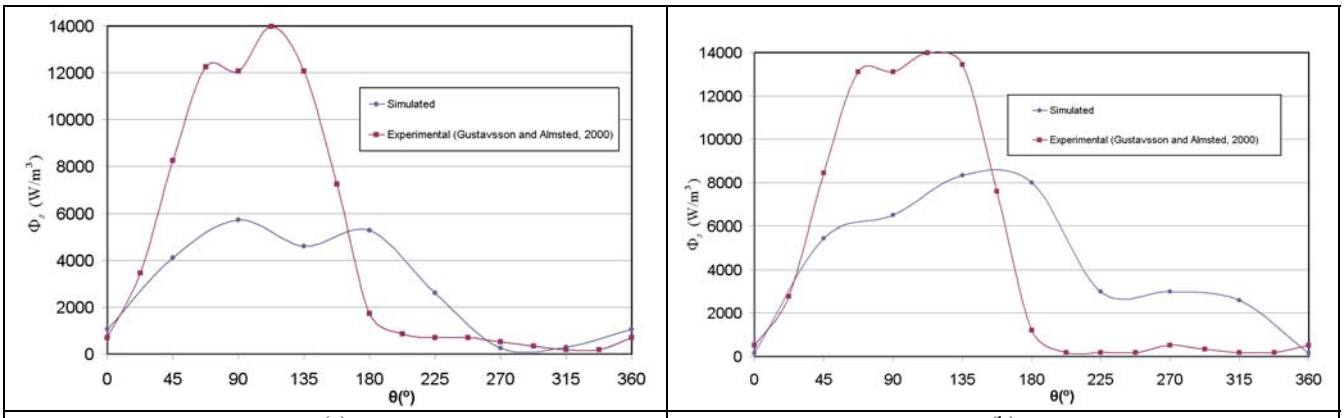

Figure 8. Simulated kinetic energy dissipation at various circumferential angular positions in the surface of the tube and values from experimental results by Gustavsson and Almstedt, 2000. Operational pressures : (a) 0.8 MPa ; (b) 1.6 MPa

Figure 8 shows a comparison between the numerically predicted time averaged values of the kinetic energy dissipation rate, using the baseline simulation models discussed in section 4, and those based on the experimental values for the T2 arrangement in the work of Gustavson and Almstedt (2000). The complete description of experimental conditions for the T2 arrangement can be found in the mentioned work. A comparison of the numerical and experimental results for the two different operational pressures (c.f. Figs 8(a) and 8(b)) shows some degree of discordance. However, the lack of minutely agreement with experimental values, the results can be compared for recognizing similar drifts. For instance, from the Fig 8, the higher simulated values of the dissipation rate occurring in

the bottom position of the tube, i.e. for $\theta < 180^o$, is in agreement with the experimental counterpart. Similarly, the increase of dissipation rate with increased operational pressure for the simulated results is in agreement with the experimental values. Regarding the erosion and baseline models used for the simulation, some remarks towards better agreement with experimental values can also be done. According to the monolayer erosion model and its discussion above Eq. (19) some degree of uncertainty is associated to the multiplying constant, as the exact value of elasticity of collision is not known. It is also expected, that adjustments in the baseline simulation models, such as those outlined in Figs. (4) to (6) would produce better agreement.

6. CONCLUSIONS

In this work was investigated numerically the hydrodynamics of a two dimensional bed with an immersed tube. The objective of these study was two fold : explore and investigate some effects not previously explored in the literature, to verify the feasibility of the MFIX code for such a kind of study. Our results points to significant influences in the predicted dissipation rates and consequently, in the erosion rate, when employing different drag models. The dissipation rate is also influenced by either the use of blending functions for the transition between the plastic and viscous regime of solids flow or the use of a constant viscosity model. The results are key sensitive to the slip condition for the gas phase in the surface of the tube. In the case of a free slip condition for the gas phase the lowest values of dissipation are obtained. The geometric effect study also pointed some interesting conclusions. Increase the bed width, decreases the dissipation rate, and the placement of the tube at a height where the bubble can grow sufficiently to encompass the tube results in greater dissipation rate. Finally, a preliminary comparison with experimental data by Gustavsson and Almstedt (2000) reveals the simulation values are smaller than the experimental measured. In spite of this, the two results show grossly similar trends.

7. ACKNOWLEDGEMENTS

The support from MFIX users forum and CENAPAD-SP is gratefully acknowledged

8. REFERENCES

Achim, D., Easton, A. K., Schwarz, M. P., Witt, P.J., Zakhari, A., 2002, “Tube erosion modelling in a fluidised bed”, Applied Mathematical Modelling, Vol 26, pp. 191-201.

Anderson, T. B., 1967, “A fluid mechanical description of fluidized beds: Equations of motion”, Industrial Engineering Chemical Fundamentals, Vol 6, pp. 527-539.

Benyahia, S., 2008, “Validation study of two continuum granular frictional flow theories”, Industrial Engineering Chemical Research, 47, 8926-8932.

Benyahia, S., Syamlal, M., O’Brien, T. J., “Summary of MFIX Equations 2005-4”, 1 March 2006: <http://www.mfix.org/documentation/MfixEquations2005-4-1.pdf>.

Benyahia, S., Syamlal, M., O’Brien, T. J., 2006, “Extension of Hill–Koch–Ladd drag correlation over all ranges of Reynolds number and solids volume fraction”, Powder Technology, 162, 166-174.

Bouillard, J. X., Lyczkowski, R. W., 1991, “On the erosion of heat exchanger tube banks in fluidized-bed combustor”, Powder Technology, Vol 68, pp. 37-51.

Cebeci, T., Shao, J. P., Karyeke, F., Laurendeau, E., 2005, Computational Fluid Dynamics for Engineers, Horizon Publishing Inc, USA, 402p.

Enwald, H., Peirano, E., Almstedt, A. E., Leckner, B., 1999, “Simulation of the fluid dynamics of a bubbling fluidized bed: Experimental validation of the two-fluid model and evaluation of a parallel multiblock solver”, Chemical Engineering Science, 54, 311-328.

Ergun, S., 1952, “Fluid-flow through packed columns”, Chemical Engineering Progress, Vol 48, n. 2, pp. 91-94.

Fan, J. R., Sun, P., Chen, L. H., Cen, K. F., 1998, “Numerical investigation of a new protection method of the tube erosion by particle impingement”, Wear, Vol 223, pp. 50-57.

Gustavsson, M., Almstedt, A. E., 1999, “Numerical simulation of fluid dynamics in fluidized beds with horizontal heat exchanger tubes”, Chemical Engineering Science, 55, 857-866.

Gustavsson, M., Almstedt, A. E., 2000, “Two-fluid modelling of cooling-tube erosion in a fluidized bed”, Chemical Engineering Science, 55, 867-879.

He, Y. R., Lu, H. L., Sun, Q. Q., Yang, L. D., Zhao, Y. H., Gidaspow, D., Bouillard, J., 2004, “Hydrodynamics of gas-solid flow around immersed tubes in bubbling fluidized beds”, Powder Technology, 145, pp. 88-105.

He, Y. R., Zhan, W., Zhao, Y., Lu, H. Schlaberg, I., “Prediction on immersed tubes erosion using two-fluid model in a bubbling fluidized bed”, Chemical Engineering Science, 64, pp. 3072-3082.

Hill, R. J., Koch, D. L., Ladd, J. C., 2001, “Moderate-Reynolds-number flows in ordered and random arrays of spheres”, Journal of Fluid Mechanics, Vol 448, p. 243-278.

Hill, R. J., Koch, D. L., Ladd, J. C., 2001, "The first effects of fluid inertia on flows in ordered and random arrays of spheres", Journal of Fluid Mechanics, Vol 448, pp. 213-241.

Kobayashi, N., Yamazaki, R., Mori, S., 2000, "A study on the behaviour of bubbles and solids in bubbling fluidized beds", Powder Technology, Vol 113, pp. 327-344.

Lathowers, D., Bellan, J., 2000, "Modeling of dense gas-solid reactive mixtures applied to biomass pyrolysis in a fluidized bed", Proceedings of the 2000 U.S. DOE Hydrogen Program Review, NREL/CP-570-28890. USA.

Lee, S. W., Wang, B. Q., 1995, "Effect of particle-tube collision frequency on material wastage on in-bed tubes in the bubbling fluidized bed combustor", Wear, Vol 184, pp. 223-229.

Lyczkowski, R. W., Bouillard, J. X., 2002, "State-of-the-art review of erosion modeling in fluid/solid systems", Progress in Energy and Combustion Science, Vol 28, pp. 543-602.

Ozawa, M., Umekawa, H., Furui, S., Hayashi, K., Takenaka, N., 2002, "Bubble behavior and void fraction fluctuation in vertical tube banks immersed in a gas-solid fluidized-bed model", Experimental Thermal and Fluid Science, Vol 26, pp. 643-652.

Pannala, S., Daw, C. S., Finney, C. E. A., Benyahia, S., Syamlal, M., O´Brien, T. J., "Modelling the collisional-plastic stress transition for bin discharge of granular material", 2009, Powders and Grains 2009 – Proceeding of the 6th International Conference on Micromechanics of Granular Media, pp. 657-660.

Schaeffer, D. G., 1987, "Instability in the evolution equations describing incompressible granular flow", Journal Differential Equations, v. 66, pp. 19-50.

Siravastava, A., Sundaresan, S., 2003, "Analysis of a frictional–kinetic model for gas–particle flow", Powder Technology, v. 129, pp. 72-85.

Syamlal, M., 1998, "MFIX Documentation, Numerical Techniques", Technical Note, DOE/MC-31346-5824, NTIS/DE98002029, National Technical Information Service, Springfield, VA, USA.

Syamlal, M., Rogers, W. A., O'Brien, T. J., 1993, "MFIX Documentation, Theory Guide", Technical Note, DOE/METC-94/1004, NTIS/DE94000087, National Technical Information Service, Springfield, VA, USA.

Wang, A. L. T., Clough, S.J., Stubington, J. F., 2002, "Gas flow regimes in fluidized-bed combustors", Proceedings Combustion Institute, Vol 29, pp. 819-826.

Wang, J., van der Hoef, M. A., Kuipers, J. A. M., 2010,"CFD study of the minimum bubbling velocity of Geldart A particles in gas-fluidized beds", Chemical Engineering Science, 65, pp. 3772-3785.

Wen, C. Y., Yu, Y. H., 1966, "Mechanics of Fluidization", Chemical Engineering Progress Symposium Series, Vol 62, n. 62, pp. 100-111.

Wiman, J., 1994, An experimental study of hydrodynamics and tube erosion in a pressurized fluidized with horizontal tubes. Thesis for the degree of Licentiate of Engineering, Chalmers University of Technology, Goteborg. Sweden.

Wiman, J., Almstedt, A. E., 1997, "Hydrodynamics, erosion and heat transfer in a pressurized fluidized bed: influence of pressure, fluidization velocity, particle size and tube bank geometry", Chemical Engineering Science, Vol 52, pp. 2677-2695.

Wong, Y. S., Seville, J. P. K., 2006, "Single-particle motion and heat transfer in fluidized beds", AIChe Journal, Vol 52, pp. 4099-4109.

5. RESPONSIBILITY NOTICE

The authors are the only responsible for the printed material included in this paper.